

Catalysis Science & Technology

Accepted Manuscript



This article can be cited before page numbers have been issued, to do this please use: K. Park, S. Lim, J. H. Baik, H. Kim, K. Jung and S. Yoon, *Catal. Sci. Technol.*, 2018, DOI: 10.1039/C8CY00294K.



This is an Accepted Manuscript, which has been through the Royal Society of Chemistry peer review process and has been accepted for publication.

Accepted Manuscripts are published online shortly after acceptance, before technical editing, formatting and proof reading. Using this free service, authors can make their results available to the community, in citable form, before we publish the edited article. We will replace this Accepted Manuscript with the edited and formatted Advance Article as soon as it is available.

You can find more information about Accepted Manuscripts in the [author guidelines](#).

Please note that technical editing may introduce minor changes to the text and/or graphics, which may alter content. The journal's standard [Terms & Conditions](#) and the ethical guidelines, outlined in our [author and reviewer resource centre](#), still apply. In no event shall the Royal Society of Chemistry be held responsible for any errors or omissions in this Accepted Manuscript or any consequences arising from the use of any information it contains.



Journal Name

ARTICLE

Exceptionally Stable Rh-based Molecular Catalyst Heterogenized on a Cationically charged Covalent Triazine Framework Support for Efficient Methanol Carbonylation

Received 00th January 20xx,
Accepted 00th January 20xx

DOI: 10.1039/x0xx00000x

www.rsc.org/

Kwangho Park^{a†}, Sangyup Lim^{a†}, Joon Hyun Baik^b, Honggon Kim^c, Kwang-Deog Jung^c, and Sungho Yoon^{*†}

Direct carbonylation of methanol into methyl acetate and acetic acid using Rh-based heterogeneous catalysis is of great interest due to the effective levels of activity and stability. Here, a Rh-based molecular catalyst heterogenized on a charged 1, 3-bis(pyridyl) imidazolium-based covalent triazine framework (Rh-bpim-CTF) was synthesized and characterized to have a single-site distribution of metal molecular species throughout the support by its ligation to abundant N atom sites. Methanol carbonylation was performed using the Rh-bpim-CTF catalyst in plug-flow reaction in gas phase, affording a turnover frequency up to 3693 h⁻¹ and productivity of 218.9 mol kg⁻¹ h⁻¹ for acetyl products with high stability.

Introduction

Acetic acid (AA) and methyl acetate (MA) are highly versatile organic compounds that find wide applications ranging from basic solvents for industrial processes to reagents for manufacturing more value-added materials such as polymers and fibers.¹ In particular, MA has garnered recent interest as an alternative carbon feedstock for its conversion into ethanol via hydrogenation and for cell growth in biotechnology.²⁻⁶ AA and MA can be produced via a number of synthetic routes, typically dimethyl ether (DME) or methanol carbonylation. However, the DME carbonylation is still under development because its low efficiency hinders its industrialization.⁷

Methanol carbonylation using Rh- and Ir-based catalysts stands out as the more relevant industrial process for the worldwide production of AA and MA; it is successfully applied by many chemical companies in homogeneous systems, i.e., the Monsanto and Cativa processes, as well as in heterogeneous systems, i.e., the Acetica and BP SaaBre processes.⁸⁻¹² However, despite reaching effective levels of activity, the homogeneous systems present a major drawback. Such systems increase the complexity and cost of the manufacturing process such as the recycling of catalyst from corrosive product mixture.⁹ In contrast, in heterogeneous systems, the catalysts are

segregated from the reaction mixture and can be used in continuous liquid- and gas-phase reactions. In particular, the total economic cost can be reduced if the products can be easily separated from the catalysts in gas-phase reaction process.^{11, 12} However, the development of heterogeneous catalysts with high efficiency and long-term stability is considerably challenging nowadays because of the efficiency gap between homogeneous and heterogeneous systems.

The development of novel heterogeneous catalytic systems via the heterogenization of molecular metal complexes on various catalytic supports has achieved remarkable progression.¹³⁻²⁴ The well-defined ligand sites on the supports in Rh-catalyzed methanol carbonylation could provide abundant binding sites for the metal complexes and enhanced the nucleophilicity of the Rh(I) active site, thereby increasing the catalytic activity in such reactions. In particular, the positively charged ligand structures on the surface of the support could dramatically increase the stability of the catalyst even at high temperatures and pressures via the electrostatic interaction with the catalytic active species, i.e., [Rh(I)CO₂I₂]⁻. In this context, devising novel heterogeneous catalyst supports with the aim of increasing the catalytic efficiency of manufacturing processes is currently garnering substantial interest in the industrial fields.

Recently, covalent triazine frameworks (CTFs) have garnered increasing attention as catalytic supports because they constitute a highly porous structure with robustness under high pressure, thermal, and chemical conditions (i.e., acidic or basic).²⁵⁻³⁶ In particular, CTFs possess abundant nitrogen-based basic ligand sites that function similar to those in homogeneous ligands. Upon heterogenization with a metal complex, CTFs afford strong coordination sites and provide the metal center with σ -donor capability. Furthermore, recent reports

^aDepartment of Bio & Nano Chemistry Kookmin University 861-1 Jeongneung-dong, Seongbuk-gu, Republic of Korea

^{*}Corresponding Author, Sungho Yoon. E-mail: yoona@kookmin.ac.kr

^bClimate and Energy Research Group, Research Institute of Industrial Science & Technology (RIIST), 67 Cheongam-ro, Pohang 37673, Republic of Korea.

^cClean Energy Research Centre, Korea Institute of Science and Technology, P.O. Box 131, Cheongryang, Seoul 136-791, Republic of Korea.

[†]These authors contributed equally

Electronic Supplementary Information (ESI) available: See DOI: 10.1039/x0xx00000x

illustrate that the incorporation of ionic building blocks on the CTFs resulted in high level of homogeneous charge distribution

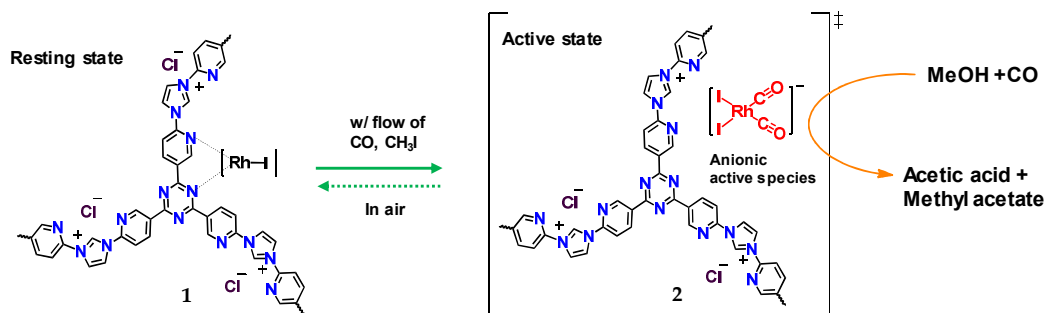


Figure 1 Structural representations of Rh-bpim-CTF catalyst in resting state under ambient atmosphere (1) and the suggested structure of in situ generated active state under the carbonylation conditions. (2).

on the surface.^{37, 38} The charged CTFs could tightly bind anionic complexes in various reaction conditions via ion-pair interaction, thereby showing high potential as catalytic supports.^{39, 40}

The first-ever synthesis and characterization of a Rh-based single-site catalyst heterogenized on a charged 1,3-bis(pyridyl)imidazolium-based CTF support (Rh-bpim-CTF) for its application in the carbonylation of methanol in a continuous plug-flow reaction system in the gas phase is presented herein. The catalytic species was implemented as a single-site catalyst distributed via the support by its ligation to abundant N atom sites (Figure 1, 1). As a result of the high electron donation from the N-rich environment of the pore surface, the Rh-bpim-CTF catalyst featured higher efficiency compared with other heterogeneous catalytic systems. Moreover, the long-term stability of the catalyst during the continuous process was confirmed: perceptible catalytic deactivation was not detected, which is most likely caused by the strong ion-pair interaction between the positive-charged [imidazolium]⁺ moiety and the catalytic active species $[\text{Rh}(\text{CO})_2\text{I}_2]^-$ (Figure 1, 2).

Experimental

Materials and methods

All chemicals were purchased from commercial suppliers and used without further purification. 2-Bromo-5-cyanopyridine (99%) was purchased from T.C.I. chemicals. 1-Methyl-1H-imidazole (99%) and zinc chloride (98%) were purchased from Sigma Aldrich. Methanol, methyl iodide were purchased from DAEJUNG. Rhodium(III) chloride was purchased from Alfa Aesar. Rh(I) carbonyl iodide dimer was synthesized as per a previous report.⁴¹ The mixture of CO and N₂ (9:1 ratio) was obtained from Sinyang gas industries.

Fourier-transform infrared (FT-IR) analysis was performed on a Nicolet iS 10 (Thermo Fisher Scientific) using KBr pellet. scanning electron microscopy (SEM) and energy-dispersive spectroscopy (EDS) were performed on a JEOL LTD (JAPAN) JEM-7610F operated at an accelerating voltage of 20.0 kV. N₂ adsorption and desorption measurements were conducted at 77 K using a BELSORP mini II (JAPAN). The samples were degassed for 1 day at 200°C before the measurements. X-ray photoelectron Spectroscopy (XPS) analysis was performed on ESCA 2000 (VG microtech) at a pressure of $\sim 3 \times 10^{-9}$ mbar using

Al K α as the excitation source ($h\nu=1486.6$ eV) with concentric hemispherical analyzer. Rh content was determined by an inductively coupled plasma optical emission spectroscopy (ICP-OES) using iCAP 6000 (Thermo scientific, USA). The Diffuse Reflectance Infrared Fourier Transform (DRIFT) spectra were obtained by using Nicolet 6700 (Thermo Electron Co.) equipped with an MCT detector and the Praying MantisTM high temperature reaction chambers (Harrick Scientific Products Inc.). The sample was pre-heated before the measurements at 200°C for 1 h to remove the moisture captured inside of the support. Elemental analysis (EA) was performed with an elemental analyser (Vario Micro cube, Germany). Transmission electron microscopy (TEM) analyses were performed on a Jeol JEM-2100F HRTEM and operated at 200 kV. The samples were prepared by dispersing with Ethanol and placed on a holey carbon film grid by dropping. After dried under vacuum at 60°C, samples were analysed in both bright field and dark field imaging modes.

Synthetic procedures

Synthesis of bpim-CTF support. The bpim-CTF was prepared according to the previously reported procedure.³⁵ In a glove box, 1,3-bis(5-cyanopyridyl)imidazolium bromide (bpim) (1.00 g, 2.83 mmol) and zinc chloride (1.89 g, 14.2 mmol) were charged into an 50 ml of ampoule and flame sealed under vacuum, which is heated to 500°C in a furnace with heating rate of 1°C min⁻¹ and maintained for 48h. The crude product was ground finely and stirred with 400 mL of 1M aqueous HCl solution for 3h. Then the black solid was filtered and extensively washed with 100 mL of water and acetone for five times. The resulting solid was refluxed with 1M HCl (250 mL) for overnight, then filtered and washed with 1M of HCl (3 x 100 mL), H₂O (3 x 100 mL), THF (3 x 100 mL) and acetone (3 x 100 mL). Finally, the obtained black powder was dried under vacuum at 200°C for 6 h.

Synthesis of Rh-bpim-CTF 5.00 g of bpim-CTF and 139 mg of $[\text{Rh}(\text{CO})_2\text{I}_2]$ (1 Wt%) was charged into 250 ml round bottom flask. Then 150 ml of anhydrous methanol was added to the mixture and stirred for overnight under CO atmosphere. After the reaction finished, the resulting powder was filtered and

washed with methanol (200 ml x 5). Finally collected black powder was dried under vacuum for overnight.

Typical carbonylation procedure Methanol carbonylation was carried out in homemade stainless steel bar-type reactor. In a typical run, the Rh-bpim-CTF (200 mg) was fixed on the middle of reactor by filling the remaining empty space with glass wools and beads. After flushing with CO, the reactor was pressurized to the desired pressure (7.5-15 bar) with feed gas (CO:N₂=9:1) flow of 100 ml min⁻¹ and heated at 150-270°C before the reaction. The pressure was maintained at the desired pressure using back-pressure regulator and then gas flow rate was controlled by the mass transfer controller (14.5-58 ml min⁻¹). Methanol and methyl iodide (molar ratio of 10:1) were mixed preliminarily and supplied to the reactor using high-pressure liquid pump (0.186-0.744 ml h⁻¹). The liquid product was collected and analyzed with gas chromatography (TCD detector, series 6000, Younglin & Co.). The gas product was analyzed with an on-line GC (FID detector, series 6000, Younglin & Co.).

Results and discussion

The bpim-CTF support was synthesized as per a previous report³⁸. Briefly, bpim-CTF was synthesized by trimerization of monomer in ionothermal reaction with ZnCl₂ as Lewis acid as well as solvent at 500°C for 48 h. The afforded black powder was extensively washed and refluxed with diluted HCl and organic solvents to remove the ZnCl₂, featuring moderate chemical stability in acidic condition. The porous and N-rich characters of the bpim-CTF support were verified via SEM, EDS, FT-IR spectroscopy, and EA (Figure S1, S2, and Table S1).

In particular, the FT-IR results exhibited the broad peaks in the range at 1,450-1,650 cm⁻¹ and 1,000-1,400 cm⁻¹, which is due to the partial graphitization experienced during the synthetic procedure. However, the peaks still included the regional peaks for the triazine and imidazolium, i. e., 1,450-1,600 cm⁻¹ (C=N or C=C) and 1,200-1,400 cm⁻¹ (C-N or C-C), indicating their presence in the bpim-CTF support. Further, bpim-CTF support synthesized at 500°C was used only despite the partial thermal loss of functional groups, due to the high porosity. Initially, the bpim-CTF support was synthesized at 400 °C and used for catalyst preparation (Table S2). However, the efficiency for methanol carbonylation with the catalyst was low, which may be attributed to limited mass transfer of gas phase feed reagents to the catalytic active site due to the low porosity.

The catalyst was prepared by treating the dimer of Rh carbonyl iodide, [Rh(CO)₂I]₂, with the bpim-CTF support dispersed in methanol under CO atmosphere; this reaction afforded a black powder. SEM analysis of the thus-prepared catalyst revealed irregular block-shaped morphologies (>10 μm) (Figure 2, top left). ICP-OES analysis was performed to determine the precise loading amount of Rh in the catalyst, which was determined to be 0.61 wt% of Rh (Table 1). Brunauer-Emmett-Teller (BET) surface area analysis revealed the presence of Rh complex in the CTF supports. Thus, the surface area and pore volume of the catalyst was found to decrease after metalation

Table 1 Porosity parameters and the inductively coupled plasma-optical emission spectroscopy (ICP-OES) analysis result for the support and the Rh-bpim-CTF catalyst.

	a _{s,BET} [m ² g ⁻¹]	V _{pore, tot} ^a [cm ³ g ⁻¹]	V _{mean} ^a [nm]	ICP _{Rh} [wt%]
bpim-CTF	1764	0.84	1.91	-
Rh-bpim-CTF	1651	0.79	1.91	0.61

^aDetermined by t-plot analysis.

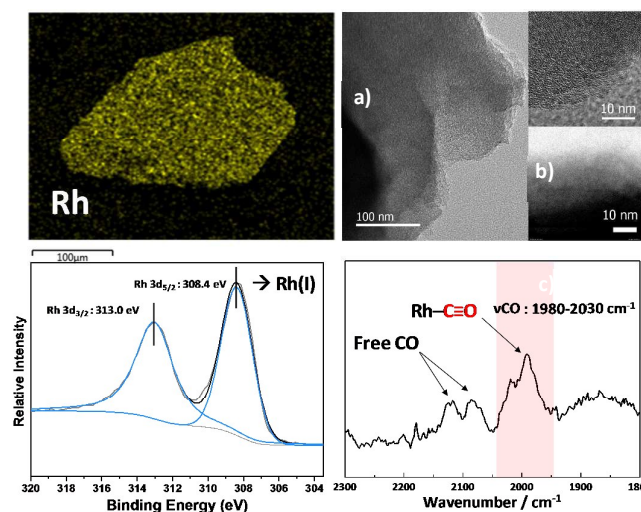


Figure 2 EDS mapping of the Rh atoms (top left), HR-TEM images (top right, a and b), and HAADF-STEM image (top right, c) for the Rh-bpim-CTF catalyst. Rh 3d XPS spectra (bottom left) and the DRIFT spectroscopy analysis result under a CO flow (bottom right) for the Rh-bpim-CTF catalyst.

from 1763 m² g⁻¹ and 0.84 cm³ g⁻¹ to 1651 m² g⁻¹ and 0.79 cm³ g⁻¹, respectively, indicating a partial occupation of the pore by the ligated Rh complex in the framework (Table 1). It is nonetheless worth mentioning that the catalyst still exhibits enough porosity for the reagents to access the active metal site.

Furthermore, an EDS analysis was performed to confirm the distribution state of Rh on the support. A homogenous distribution of Rh throughout the framework was found, suggesting the uniform ligation of Rh metal center to the abundant N- binding sites (Figure 2, top right). In addition, iodine was also homogeneously distributed throughout the framework, indicating the formation of a RhI complex (Figure S3).

High-resolution transmission electron microscopy (HR-TEM) and high-angle annular dark-field scanning transmission electron microscopy (HAADF-STEM) analysis were performed to understand the dispersion state of Rh complex (Figure 2, top right). However, the detection of the Rh single atoms on the bpim-CTF support was unsuccessful. Meanwhile, it has been reported that Rh atoms can be reduced to zero-valent metal nanoparticles in the preparation steps.¹⁶ Consequently, the HR-TEM image showed that no nanoparticle was found in the Rh-bpim-CTF catalyst with different magnifications. HAADF-STEM analysis revealed the same result.

XPS analysis was performed to precisely elucidate the chemical state of the compositions in the catalyst, and the results

ARTICLE

Journal Name

were referenced relative to the C1s value (284.6 eV, C-C). The deconvoluted C 1s spectrum was fitted using four peaks with electron-binding energy (EBE) of 284.6 eV (C–C/C–H species), 285.4 eV (C–N species), 286.5 eV (C–O species), and 288.2 eV (O–C=O species), (Figure S6, top left). Similarly, the deconvoluted N 1s spectrum consists of four peaks with binding energy with 398.8 eV (pyridinic N species), 400.0 eV (pyrrolic N species), 401.1 eV (quaternary N species), and 403.3 eV (oxidized N–O species), (Figure S6, top right).³⁹ The peaks are attributed to the triazine, pyridine, and imidazolium in bpim-CTF, which is binding site with Rh species. Further, to elucidate the change of electronic environment of the Rh around the bpim-CTF support, Rh-bpim-CTF and other Rh species, i.e., [Rh(CO)₂I]₂ and RhCl₃ were also confirmed (Figure 2, bottom left and Figure S6 bottom left and right). The Rh 3d_{5/2} EBE was found to be 308.4 eV, 308.7 eV, and 309.8 eV respectively. Thus, the results proved that EBE of Rh on bpim-CTF support was similar to [Rh(CO)₂I]₂, which can be inferred to Rh(I) oxidation state (Figure 2, bottom left).^{42, 43} Moreover, this EBE value decreased by 0.3 eV from that of [Rh(CO)₂I]₂, which is most likely caused by the increased electron density in the Rh center owing to the electron donation from the N-rich bpim-CTF support. XPS measurements also showed the Rh/I atomic ratio to be 1:1.26 (Table S3), indicating the formation of a RhI complex incorporated on the bpim-CTF support.

Meanwhile, an IR spectroscopy analysis was performed to track the presence of CO in the Rh-bpim-CTF catalyst using KBr pellet. The results revealed the absence of CO; the loss of CO may have occurred in ambient atmosphere (Figure S7). However, a diffuse reflectance infrared Fourier transform (DRIFT) spectroscopy analysis under a CO flow exposed the presence of CO peaks in the region of 1980–2030 cm⁻¹, which are the characteristics of the symmetric and asymmetric stretching of a terminal CO ligand (Figure 2, bottom right). This result confirms that the incorporated Rh complex readily provided the appropriate coordination site for free CO, thereby constituting the catalytic active species in the methanol carbonylation process.

In a typical methanol carbonylation experiment, the catalyst was fixed at the center of the stainless-bar reactor (Figure S8); the catalyst was then pressurized up to targeted pressure (7.5–15 bar) with CO and heated to targeted temperature. After reaching the targeted level, the pressure was controlled using a back-pressure regulator under a continuous flow of a mixture of CO and N₂ (9:1) with desired feed flow rate. Methanol and methyl iodide were preliminarily mixed in liquid phase (10:1 molar ratio) and supplied to the reactor using a high-pressure liquid pump following the feed flow conditions (Table S4). The liquid phase reagents were pre-heated up to 240°C to their vapor phase and subsequently mixed with the CO before they entered the reactor. The gas-phase reaction media was cooled down after passing through the reactor to be collected in the liquid form.

To evaluate the effect of the temperature on the Rh-bpim-CTF catalytic carbonylation, the reactions were performed in the temperature range of 150°C–270°C at 10 bar and with a

Table 2. Catalytic performances of the Rh-bpim-CTF under various reaction conditions.^a

Entry	W/F _m ^b	T	P ^c	Conv. ^d	TOF ^e	Produc. ^f	Select. ^d	
	g h mol ⁻¹	[°C]	[bar]	MeOH [%]	[mol _{AcOR} mol _{Rh} ⁻¹ h ⁻¹]	[mol _{AcOR} kg _{Cat} ⁻¹ h ⁻¹]	MA [%]	AA [%]
1	3.8	150	10	10.3	457	27.1	88.0	12.0
2	3.8	180	10	24.8	1101	65.2	94.3	5.7
3	3.8	210	10	47.6	2113	125.2	89.1	10.9
4	3.8	240	10	62.1	2756	163.4	75.3	24.7
5	3.8	270	10	72.5	3218	190.7	76.5	23.5
6	3.8	240	7.5	40.6	1802	106.8	89.1	10.9
7	3.8	240	12.5	77.0	3417	202.6	67.7	32.3
8	3.8	240	15	83.2	3693	218.9	62.5	37.5
9	1.9	240	10	35.7	3169	187.8	92.7	7.3
10	2.5	240	10	43.0	2863	169.7	85.8	14.2
11	7.6	240	10	94.6	2100	124.4	44.0	56.0

^aReaction conditions: 0.2 g of Rh-bpim-CTF was fixed on the stainless-bar reactor, and pressurized up to the desired pressure and temperature. ^bA ratio of catalyst weight and methanol feed gas flow, i.e., contact time. ^cTotal pressure at the desired temperature ^dConversion and Selectivity of the products were analyzed using a gas chromatography. ^eTurn over frequency (TOF) = mole of acetyl products per mole of Rh per hour at steady-state conversion. ^fProductivity = mole of acetyl products per kilogram of the catalyst per hour at steady-state conversion.

ratio of catalyst weight and methanol feed gas flow, i.e., contact time, (W/F_m) of 3.8 g h mol⁻¹ (Table 2, entry 1–5). The catalytic methanol conversion was found to be low (yield <10%) at 150°C; however, increasing the reaction temperature led to a gradual increase of the methanol conversion with 62% yield at 240°C and reached a maximum of 72.5% at 270°C, affording a TOF of 2756 and 3218 h⁻¹ respectively. MA and AA were the major products of the reaction. The effect of the reaction temperature on the selectivity of the methanol carbonylation was also considered. The selectivity for MA increased noticeably at 180°C (94.3%), whereas that for AA decreased (5.7%). As the temperature increased, the formation of AA gradually rose up to a maximum of 24.7%, and the MA formation reached a minimum of 75.3% at 240°C. Further catalytic activity tests were performed at 240°C to avoid possible deactivation of the catalyst derived by the thermal degradation of bpim-CTF support.³⁸

Additional experiments were conducted to evaluate the dependence of the catalytic activity on the pressure change (Table 2, entry 4, 6–8). A linear increase of the methanol conversion was observed as the pressure increased. Notably, such an effect was more evident at a high pressure, which may be attributed to the increased accessibility and concentration of reagents. In particular, the increased methyl iodide partial pressure imparts rate-accelerating properties to the methanol carbonylation, which is known to be the first order reaction for

methyl iodide.^{12, 44, 45} The boiling points of methanol and methyl iodide also rise at high pressures and turn the reaction into its liquid phase. Owing to this, a 10-bar pressure was adopted as the reaction condition to maintain the reaction in the gas phase.

Further reactions were investigated to evaluate the influence of the contact time of a substrate to active site on the reactivity and selectivity of the catalyst (Table 2, entry 4, 9-11). The results showed that the methanol conversion increased rapidly with W/F_m ratio = 7.6 g h mol^{-1} and reached a 94.6% conversion, reaching a TOF of 2100 h^{-1} and productivity of $124.4 \text{ mol kg}^{-1} \text{ h}^{-1}$. At the same time, it was observed that the selectivity for AA reached its maximum at 56.0% and that for MA at 44.0%. This is likely caused by an increase in the hydrolysis ratio of MA to AA with the increased reaction time.^{22, 24} The methanol conversion was almost linearly reduced to a minimum value of 35.7% at $W/F_m = 1.9 \text{ g h mol}^{-1}$ as the contact time decreased. The selectivity for AA dramatically reduced up to 7.3%; in contrast, the best MA yield of 92.7% was obtained with a TOF of 3169 h^{-1} and productivity of $187.8 \text{ mol kg}^{-1} \text{ h}^{-1}$. This efficiency was higher than that of other catalysts that were previously reported^{13, 14, 16-24}; this phenomenon can be explained in terms of the increased electron donation effects from the bpim-CTF to the Rh metal center.

Catalyst stability is one of the most significant factors to establish the potential usefulness of a catalyst industrial scale. We therefore evaluated the stability of the Rh-bpim-CTF system in the methanol carbonylation process by screening the catalytic activity under the conditions of $W/F_m = 7.6 \text{ g h mol}^{-1}$, at the temperature of 240°C , and at 10-bar pressure with continuous flow of reagents. To assess the effect of cationic charge on the bpim-CTF support, the Rh-based catalyst heterogenized on a bipyridine based CTF support (Rh-bpy-CTF) was also synthesized and used for screening the catalytic activity (Figure S10). The Rh-bpy-CTF showed less catalytic activity with the slight deactivation over time. This may be attributed to the weak binding of Rh active species during the flow reaction, resulting in leaching of metal. In contrast, the present catalyst showed consistent catalytic activity during the process (Figure 3); the Rh-bpim-CTF system showed long-term stability and high efficiency in a 40-h process. Thus, the conversion of methanol was $93.5\% \pm 1$ with selectivities of $49\% \pm 5$ for AA and of $40\% \pm 3$ for MA. This behaviour can be ascribed to the strong ion-pair interaction between the [imidazolium]⁺ moiety on the bpim-CTF support and the active species $[\text{RhI}_2\text{CO}_2]^-$, providing extra stability to the catalyst.

The thermal gravimetric analysis (TGA) results also exhibited that the overall weight of the Rh-bpim-CTF was well-maintained at the temperature of 240°C except for the slight evaporation of water in the time to raise the temperature (< 7%), featuring high thermal stability of Rh-bpim-CTF (Figure S11). Further, the catalyst was confirmed by TEM analysis after the methanol carbonylation to check the transformation of Rh atoms to nanoparticles under the catalytic reaction conditions (Figure S12). In conclusion, none of the Rh nanoparticles was observed by HR-TEM image in different magnification and by HAADF-STEM.

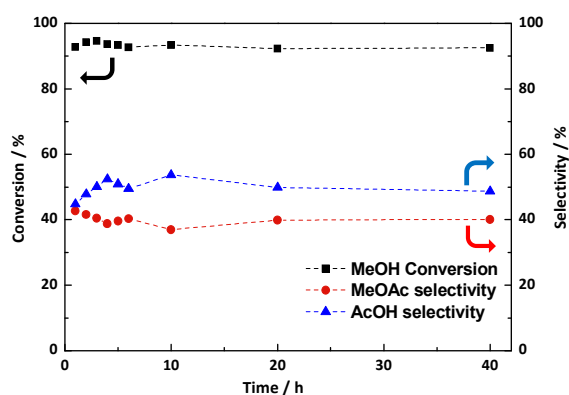


Figure 3. Stability test of the Rh-bpim-CTF for heterogeneous methanol carbonylation

Conclusions

The heterogenization of a Rh-based molecular catalyst on a charged bpim-CTF support has been explored for the carbonylation of methanol. It was found that the Rh complex was incorporated as a single-site catalyst throughout the support via the ligation between the Rh centers and the N-derived binding sites on the pore surface. The Rh-bpim-CTF catalyst exhibited an excellent catalytic conversion of methanol of 93%, corresponding to the TOF of 2100 h^{-1} and productivity of $124.4 \text{ mol kg}^{-1} \text{ h}^{-1}$ with selectivities of 56% for AA and 44% for MA at 240°C temperature, 10-bar pressure, and a W/F_m ratio of 7.6 g h mol^{-1} . Besides, in terms of methyl acetate synthesis, the selectivity for MA increased to 92.7% at a W/F_m ratio of 1.9 g h mol^{-1} , featuring TOF of 3169 h^{-1} and productivity of $187.8 \text{ mol kg}^{-1} \text{ h}^{-1}$ which constitutes an excellent value for the continuous methanol carbonylation in vapor phase. We attribute this result to the electron donation effect of the abundant N atoms on the pore surface of the CTF support. Furthermore, the CTF supported heterogeneous catalytic system exhibited an outperforming stability in a 40-h process, which is attributed to the ion-pair interaction between Rh centers and support, thereby providing extra stability to the catalyst. Thus, the proposed charged CTF is a promising candidate as a highly efficient and robust catalytic support for the continuous manufacturing process of acetyl compounds in industrial applications.

Acknowledgements

The authors acknowledge the financial support of National Research Foundation under "Next Generation Carbon Upcycling Project" (Project No. 2017M1A2A2043134) of the Ministry of Science and ICT, Republic of Korea. Gas physisorption analysis were conducted under the framework of Research and Development Program of the Korea Institute of Energy Research (KIER, B6-2434). Finally, we gratefully thank Miyeon Jang for performing SEM measurements.

References

- 1 H. Cheung, R. S. Tanke and G. P. Torrence, *Ullmann's Encyclopedia of Industrial Chemistry*, 2011.
- 2 X. Huang, M. Ma, S. Miao, Y. Zheng, M. Chen and W. Shen, *Appl. Catal., A*, 2017, **531**, 79-88.
- 3 Y. Wang, Y. Zhao, J. Lv and X. Ma, *ChemCatChem*, 2017.
- 4 X. San, Y. Zhang, W. Shen and N. Tsubaki, *Energy Fuels*, 2009, **23**, 2843-2844.
- 5 X. Li, X. San, Y. Zhang, T. Ichii, M. Meng, Y. Tan and N. Tsubaki, *ChemSusChem*, 2010, **3**, 1192-1199.
- 6 S. Choo, Y. Um, S. O. Han and H. M. Woo, *J. Biotechnol.*, 2016, **224**, 47-50.
- 7 D. Rasmussen, J. Christensen, B. Temel, F. Studt, P. Moses, J. Rossmeisl, A. Riisager and A. Jensen, *Catal. Sci. Technol.*, 2017, **7**, 1141-1152.
- 8 A. W. Budiman, J. S. Nam, J. H. Park, R. I. Mukti, T. S. Chang, J. W. Bae and M. J. Choi, *Catal. Surv. Asia*, 2016, **20**, 173-193.
- 9 C. M. Thomas and G. Süss-Fink, *Coord. Chem. Rev.*, 2003, **243**, 125-142.
- 10 G. J. Sunley and D. J. Watson, *Catal. Today*, 2000, **58**, 293-307.
- 11 Y. Noriyuki, M. Takeshi, W. Joe and S. Ben, *Stud. Surf. Sci. Catal.*, 1999, **121**, 93-98.
- 12 N. Yoneda, S. Kusano, M. Yasui, P. Pujado and S. Wilcher, *Appl. Catal., A*, 2001, **221**, 253-265.
- 13 J. S. Nam, A. R. Kim, D. M. Kim, T. S. Chang, B. S. Kim and J. W. Bae, *Catal. Commun.*, 2017.
- 14 Z. Ren, Y. Lyu, S. Feng, X. Song and Y. Ding, *Mol. Catal.*, 2017, **442**, 83-88.
- 15 G. A. Flores-Escamilla and J. C. Fierro-Gonzalez, *J. Mol. Catal. A: Chem.*, 2012, **359**, 49-56.
- 16 F. Li, B. Chen, Z. Huang, T. Lu, Y. Yuan and G. Yuan, *Green Chem.*, 2013, **15**, 1600-1607.
- 17 L. D. Dingwall, A. F. Lee, J. M. Lynam, K. Wilson, L. Olivi, J. M. Deeley, S. Gaemers and G. J. Sunley, *ACS Catal.*, 2012, **2**, 1368-1376.
- 18 M. Jarrell and B. Gates, *J. Catal.*, 1975, **40**, 255-267.
- 19 R. Sowden, M. Sellin, N. Blasio and D. Cole-Hamilton, *Chem. Commun.*, 1999, 2511-2512.
- 20 N. De Blasio, E. Tempesti, A. Kaddouri, C. Mazzocchia and D. Cole-Hamilton, *J. Catal.*, 1998, **176**, 253-259.
- 21 N. De Blasio, M. R. Wright, E. Tempesti, C. Mazzocchia and D. J. Cole-Hamilton, *J. Organomet. Chem.*, 1998, **551**, 229-234.
- 22 A. Riisager, B. Jørgensen, P. Wasserscheid and R. Fehrmann, *Chem. Commun.*, 2006, 994-996.
- 23 S. Zhang, C. Guo, Q. Qian and G. Yuan, *Catal. Commun.*, 2008, **9**, 853-858.
- 24 P. K. Saikia, P. P. Sarmah, B. J. Borah, L. Saikia and D. K. Dutta, *J. Mol. Catal. A: Chem.*, 2016, **412**, 27-33.
- 25 M. Soorholtz, L. C. Jones, D. Samuelis, C. Weidenthaler, R. J. White, M.-M. Titirici, D. A. Cullen, T. Zimmermann, M. Antonietti and J. Maier, *ACS Catal.*, 2016, **6**, 2332-2340.
- 26 K. Park, G. H. Gunasekar, N. Prakash, K. D. Jung and S. Yoon, *ChemSusChem*, 2015, **8**, 3410-3413.
- 27 A. V. Bavykina, E. Rozhko, M. G. Goesten, T. Wezendonk, B. Seoane, F. Kapteijn, M. Makkee and J. Gascon, *ChemCatChem*, 2016, **8**, 2217-2221.
- 28 R. Palkovits, M. Antonietti, P. Kuhn, A. Thomas and F. Schüth, *Angew. Chem. Int. Ed.*, 2009, **48**, 6909-6912.
- 29 P. Sudakar, G. Gunasekar, I. Baek and S. Yoon, *Green Chem.*, 2016, **18**, 6456-6461.
- 30 A. V. Bavykina, A. I. Olivos-Suarez, D. Osadchii, R. Valecha, R. Franz, M. Makkee, F. Kapteijn and J. Gascon, *ACS Appl. Mater. Interfaces*, 2017, **9**, 26060-26065.
- 31 S. Rajendiran, P. Natarajan and S. Yoon, *RSC Adv.*, 2017, **7**, 4635-4638.
- 32 K. Iwase, T. Yoshioka, S. Nakanishi, K. Hashimoto and K. Kamiya, *Angew. Chem. Int. Ed.*, 2015, **54**, 11068-11072.
- 33 A. V. Bavykina, M. G. Goesten, F. Kapteijn, M. Makkee and J. Gascon, *ChemSusChem*, 2015, **8**, 809-812.
- 34 A. V. Bavykina, H. H. Mautscke, M. Makkee, F. Kapteijn, J. Gascon and F. X. Llabres i Xamena, *CrystEngComm*, 2017, **19**, 4166-4170.
- 35 T. Yoshioka, K. Iwase, S. Nakanishi, K. Hashimoto and K. Kamiya, *J. Phys. Chem. C*, 2016, **120**, 15729-15734.
- 36 R. Kamai, K. Kamiya, K. Hashimoto and S. Nakanishi, *Angew. Chem. Int. Ed.*, 2016, **55**, 13184-13188.
- 37 O. Buyukcakir, S. H. Je, S. N. Talapaneni, D. Kim and A. Coskun, *ACS Appl. Mater. Interfaces*, 2017, **9**, 7209-7216.
- 38 K. Park, K. Lee, H. Kim, V. Ganesan, K. Cho, S. K. Jeong and S. Yoon, *J. Mater. Chem. A*, 2017, **5**, 8576-8582.
- 39 G. H. Gunasekar, K. Park, V. Ganesan, K. Lee, N.-K. Kim, K.-D. Jung and S. Yoon, *Chem. Mater.*, 2017, **29**, 6740-6748.
- 40 S. Rajendiran, K. Park, K. Lee and S. Yoon, *Inorg. Chem.*, 2017.
- 41 A. Fulford, C. E. Hickey and P. M. Maitlis, *J. Organomet. Chem.*, 1990, **398**, 311-323.
- 42 C. M. Standfest-Hauser, T. Lummerstorfer, R. Schmid, H. Hoffmann, K. Kirchner, M. Puchberger, A. M. Trzeciak, E. Mieczynska, W. Tylus and J. J. Ziolkowski, *J. Mol. Catal. A: Chem.*, 2004, **210**, 179-187.
- 43 M. C. Román-Martínez, J. A. Díaz-Auñón, C. S.-M. n. de Lecea and H. Alper, *J. Mol. Catal. A: Chem.*, 2004, **213**, 177-182.
- 44 A. Haynes, B. E. Mann, G. E. Morris and P. M. Maitlis, *J. Am. Chem. Soc.*, 1993, **115**, 4093-4100.
- 45 A. Haynes, *Adv. Catal.*, 2010, **53**, 1-45.